

## Supporting Information for “A Multilayered Approach to Complex Surface Patterning”

Peter F. Driscoll, Eftim Milkani, Christopher R. Lambert, and W. Grant McGimpsey

*Department of Chemistry and Biochemistry, Worcester Polytechnic Institute, Worcester, MA.*

### *Emission Profile of UV Lamp.*

A Rayonet reactor equipped with a 30 watt 3000 Å (300 nm) mercury lamp was used for all photo-deprotection experiments. An emission profile of the lamp is provided as Figure S1. The profile that the lamp has a broad emission profile centered slightly above 300 nm, additionally a number of sharp mercury lines are seen at higher wavelengths. It is noted that the photomasks used for surface patterning experiments cut off light below 300 nm and the lamp profile demonstrates sufficient emission above 300 nm to remove the photolabile group.

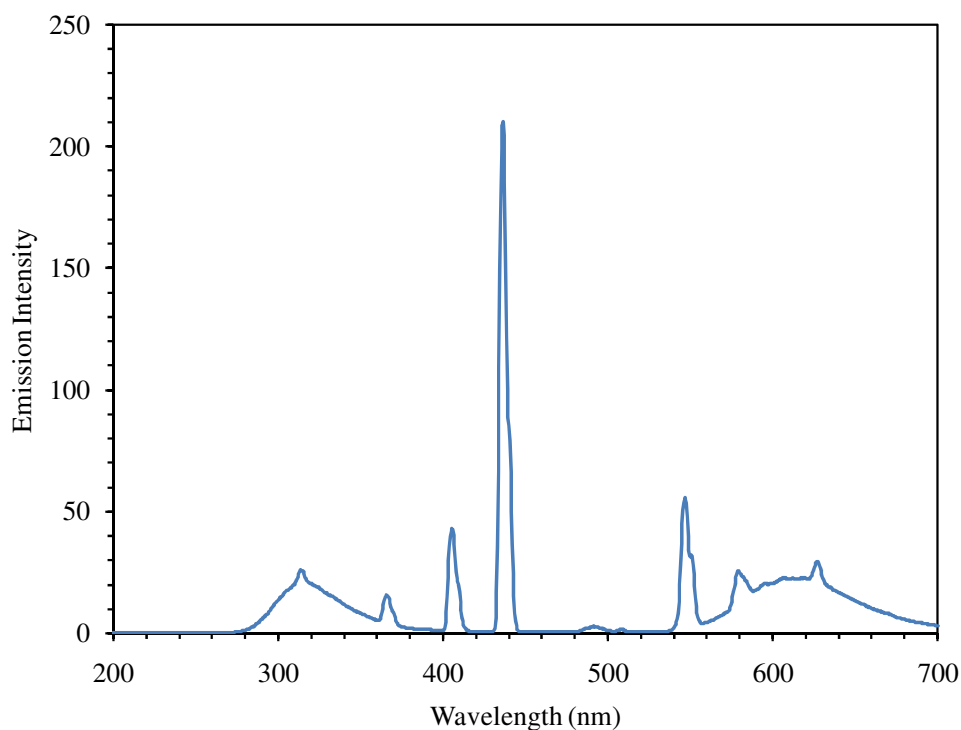


**Figure S1: Emission profile of the 300 nm lamp used for irradiation experiments.**

### *Solution Absorption and Emission Measurements.*

Absorption spectra were obtained in ethanolic solution for the photolabile compound (2-*itrobenzyl*-11-mercaptoundecanoate) before and after irradiation at 300 nm. Prior to irradiation the compound has a maximum absorbance peak at 257 nm with a shoulder extending out past 350 nm, Figure S2. Based on the absorbance data, a 300 nm lamp was chosen for irradiation experiments, and following irradiation the absorbance peak at 257 nm is no longer observed, indicating a photoreaction has occurred, Figure S3. Absorption and emission spectra of the two fluorophores used for patterning experiments, rhodamine 110 and cresyl violet 670 are shown in Figure S4. These spectra match with the excitation and emission profiles for the filter cubes used to observe the patterns with fluorescence microscopy (green: excitation filter: 460–500 nm, barrier filter: 510–560 nm, red: excitation filter: 532–587 nm, barrier filter: 608–683 nm).

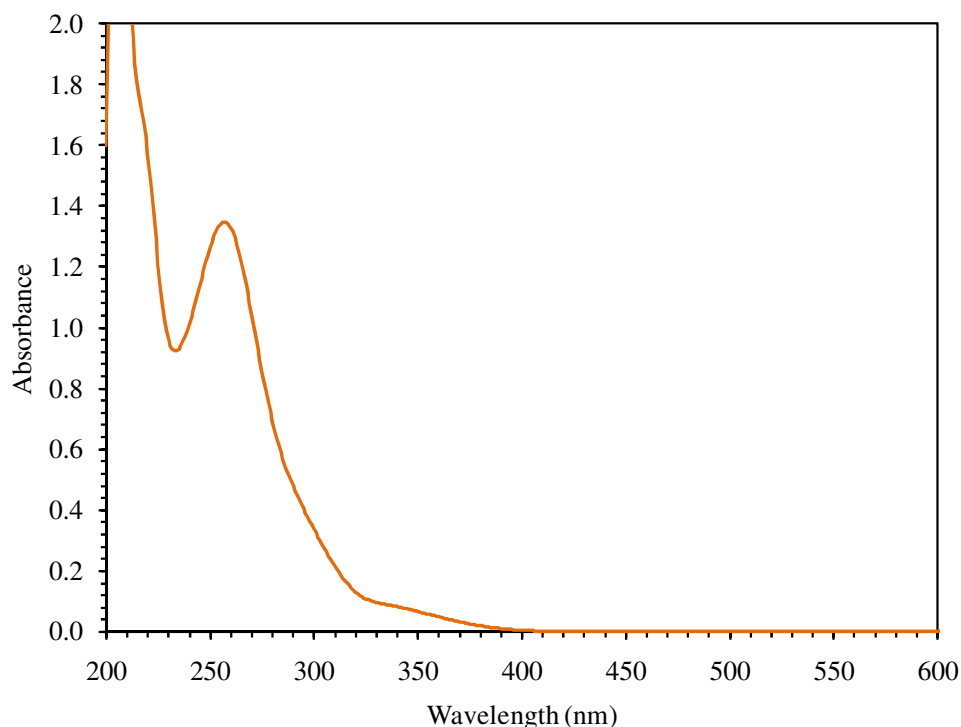


**Figure S2: Absorbance spectra of the photolabile compound in solution (EtOH).**

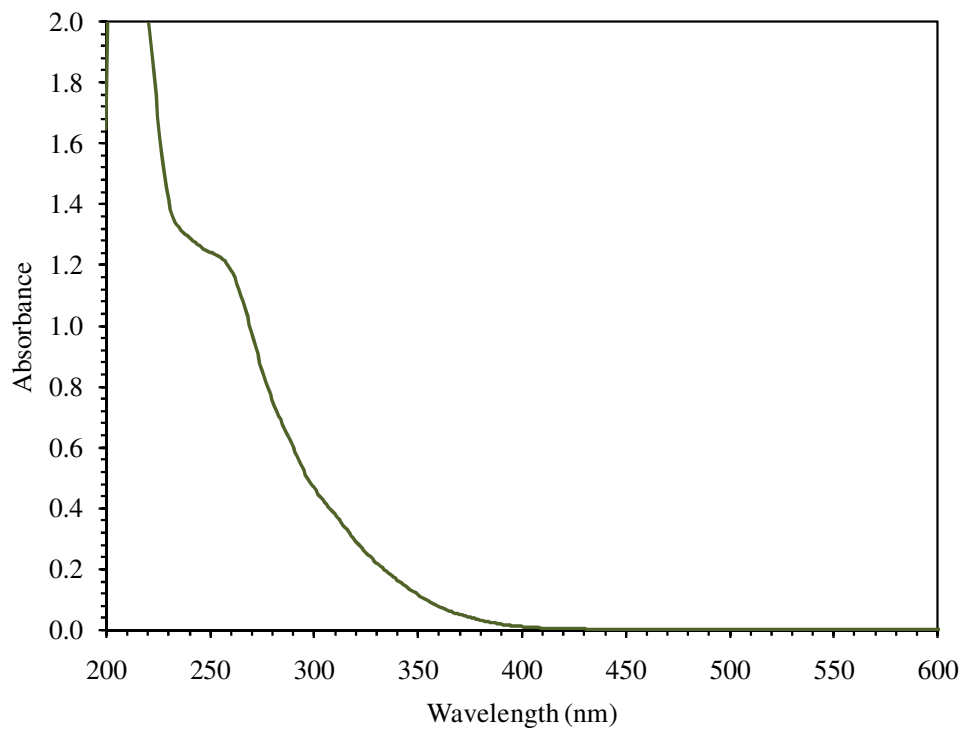


**Figure S3: Absorbance spectra of the irradiated photolabile compound in solution (EtOH).**

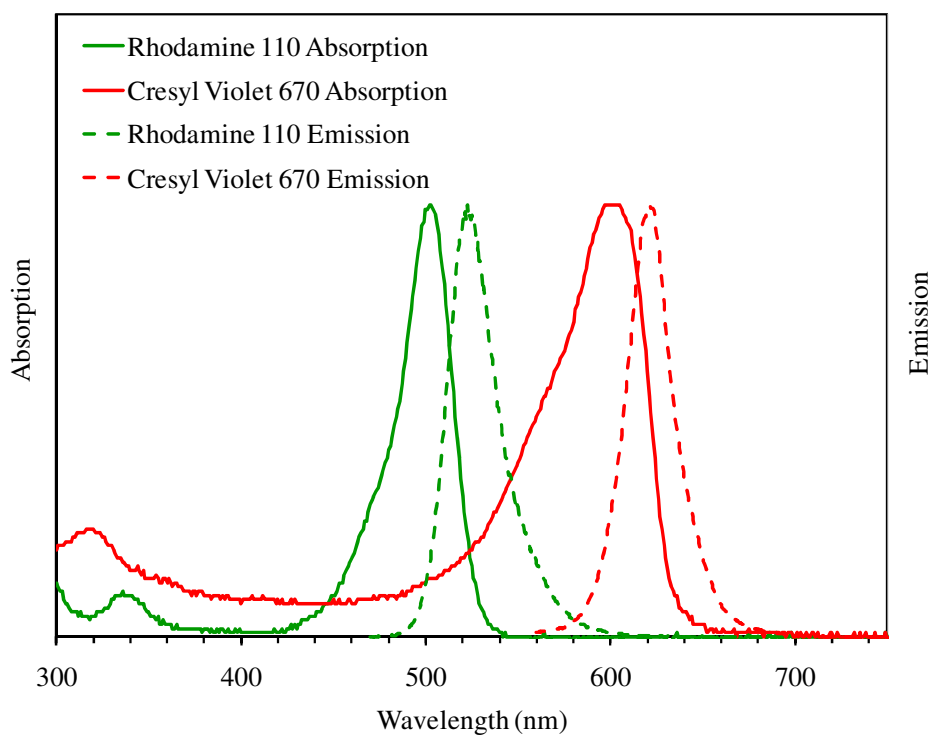


**Figure S4: Absorption and emission spectra (normalized)**

## **of rhodamine 110 and cresyl violet 670.**

### *Grazing Incidence IR.*

Grazing incidence IR shows the presence of NHS on the activated surface and also confirms that treatment with EDC/NHS does not affect the unirradiated surface, which is vital for further surface patterning. IR spectra of surfaces exposed to EDC/NHS are shown in Figure S5 (SAM – top, irradiated SAM – bottom). Analysis of the protected SAM exposed to EDC/NHS shows that the carbonyl of the ester ( $1743\text{ cm}^{-1}$ ) and the nitro group ( $1535\text{ cm}^{-1}$ ) are unchanged compared to the initial monolayer, confirming that the protected monolayer is still present on the surface. The only difference in the IR spectra between the SAM and the SAM exposed to EDC/NHS is the slight increase in the  $\text{CH}_2$  stretching frequencies of the alkyl chain. The higher wavenumbers for these signals is indicative of a more liquid-like arrangement of the alkyl chains on the surface.<sup>1</sup> This observation is likely due to the SAM being exposed to water during EDC/NHS activation; water has penetrated the film and caused the alkyl chains to lose their highly crystalline structure, however a SAM of the photolabile compound is still present. Examination of the IR spectra of the deprotected SAM exposed to EDC/NHS demonstrates that the surface has been activated (Figure S5). The signal at  $1715\text{ cm}^{-1}$  present for the deprotected monolayer has disappeared, indicating that a carboxylic acid is no longer present, as expected if the carboxylate has formed an ester bond. The three peaks and their relative intensities at  $1816\text{ cm}^{-1}$ ,  $1789\text{ cm}^{-1}$ , and  $1744\text{ cm}^{-1}$  are indicative of NHS attachment, consistent with previously published reports.<sup>2, 3</sup> Exact assignment of these signals to the different carbonyl stretching modes of the NHS functionality is somewhat controversial as both the highest and lowest frequency signals have each been assigned to the ester carbonyl stretch in different reports.<sup>3-5</sup> Most likely, the stronger absorption at  $1744\text{ cm}^{-1}$  is due to the carbonyl stretching of the NHS ester, as the peak has a similar position and intensity to that of the peak in the spectrum

of the initial monolayer, which is also a carbonyl of an ester moiety, and the surface orientation is expected to be similar. In any case, the presence of three carbonyl stretching frequencies in the intensity ratio observed in these studies is characteristic of successful NHS ester formation on the substrate. The signal at  $1646\text{ cm}^{-1}$  has been attributed to the carbonyl stretch of trace amounts of urea on the surface (the product of NHS displacing EDC in the activation step), but is more likely in this case the result of absorbed water as the substrates were thoroughly rinsed after activation.<sup>3</sup> As in the unirradiated monolayer, the  $\text{CH}_2$  stretching signals of the alkyl chain have increased in frequency, likely due to the exposure of the monolayer to water during the activation step.

IR spectra for the activated monolayer exposed to both rhodamine 110 and cresyl violet 670 are shown in Figure S6. Spectra for both of the surfaces after amide bond formation show a decrease in the  $\text{CH}_2$  stretching frequencies of the alkyl chain compared to that of the NHS activated surface, and the signals are similar to that of the monolayer which demonstrated a crystalline packing arrangement based on the IR data. A reversion to a more crystalline state is expected, due to a reorganization of the film upon exposure to the ethanolic solution that the fluorophores were deposited from. Ethanol exposure has removed water that was present after the activation step, and resulted in a similar alkyl chain orientation as was present in the monolayer. IR spectra for both fluorophore functionalized films show a prominent broad N–H stretch between  $3200\text{ cm}^{-1}$  and  $3500\text{ cm}^{-1}$ , centered at  $3370\text{ cm}^{-1}$  and  $3329\text{ cm}^{-1}$  for rhodamine 110 and cresyl violet 670 films, respectively. These signals are in the same region as the N–H stretching peaks observed in IR analysis of the bulk fluorophores (IR spectra of solid samples of both fluorescent compounds are provided below). For each film the N–H absorption is broad due to the multiple stretching modes present, each surface has a free amine as well as a newly

formed amide bond contributing to the absorption at these frequencies. Additionally, the orientation of each N–H group relative to the surface will affect the IR absorption and cannot be accurately predicted. However, each film displays a prominent N–H signal in the appropriate area of the spectrum, supporting the presence of each fluorophore on the surface. A new signal, not present in the IR spectra of either the activated substrate or the solid samples, is observed; at  $1688\text{ cm}^{-1}$  for surfaces exposed to rhodamine 110 and at  $1691\text{ cm}^{-1}$  for surfaces exposed to cresyl violet 670. These absorptions are assigned to the C=O stretch of the newly formed amide bond and are consistent with the IR absorption for carbonyls of an amide functionality (typically between  $1680\text{ cm}^{-1}$  and  $1700\text{ cm}^{-1}$ ), now present on each fluorophore modified surface. Additionally each spectra shows absorptions at approximately  $1640\text{ cm}^{-1}$  and  $1595\text{ cm}^{-1}$ , and are due to either C–N or aromatic C=C vibrations. Both fluorophore modified films retain a signal at  $1745\text{ cm}^{-1}$ , indicating that an amide bond has not formed at every possible reactive site on the surface. This observation is not surprising as both fluorophores are composed of multiple rings with considerable bulk compared to the activated surface sites, and steric hindrance will therefore limit the nucleophilic substitution reaction from occurring at each possible location. The carbonyl stretch at  $1745\text{ cm}^{-1}$  can be attributed to either remaining NHS ester moieties or hydrogen bonded carboxyl groups (if the ester has hydrolyzed), and retention of this signal has been observed in similar reports of amide bond formation using this method. It is noted that surfaces functionalized with rhodamine 110 have a broad absorption in the entire region between  $1670\text{ cm}^{-1}$  and  $1750\text{ cm}^{-1}$ . In addition to carbonyl signals for the amide and any remaining ester or (hydrogen bonded acid), rhodamine 110 also has an additional carboxylic acid functionality expected to absorb in this area which is seen at  $1703\text{ cm}^{-1}$  in the spectrum of the solid sample.

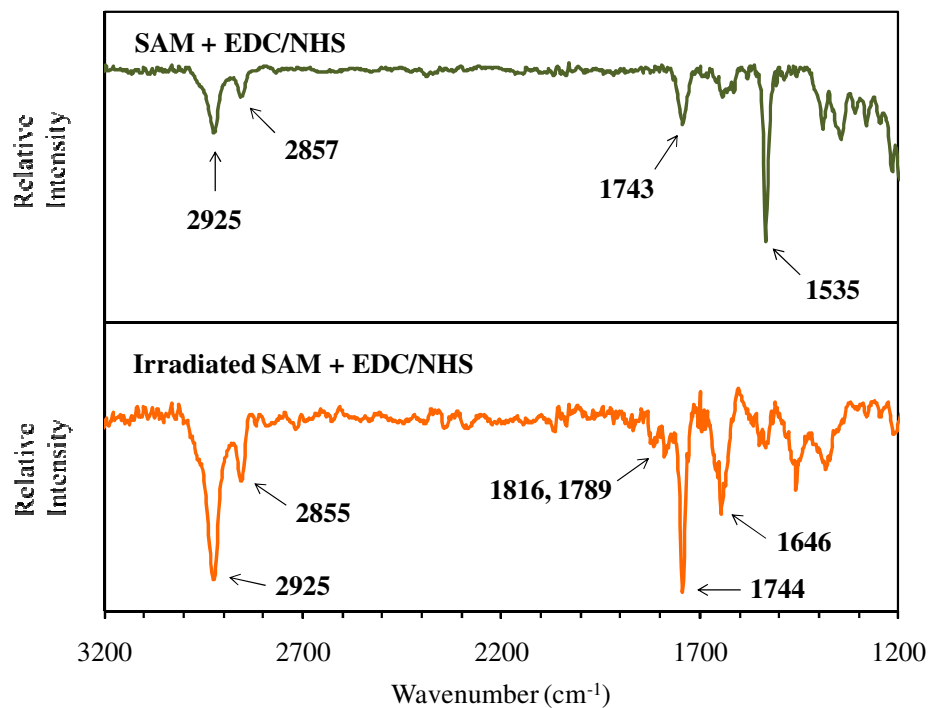


**Figure S5: Grazing incidence IR of the SAM exposed to EDC/NHS (top) and the irradiated SAM activated with EDC/NHS (bottom).**

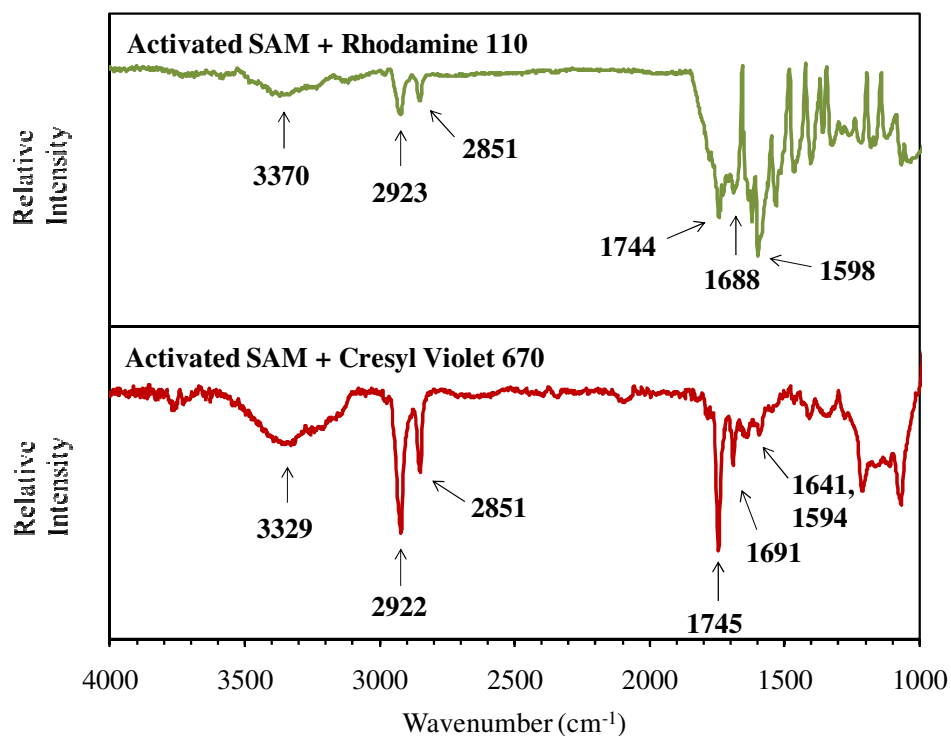


**Figure S6: Grazing incidence IR of activated monolayer after reaction with rhodamine 110 (top) and cresyl violet 670 (bottom).**

### *IR of Solid Samples (ATR).*

Infrared spectra of solid samples of each of the materials deposited on surfaces were obtained by ATR to compare to the grazing angle data acquired on the functionalized substrates. Spectra of solid samples of 2-nitrobenzyl-11-mercaptoundecanoate (photolabile compound), n-hydroxysuccinimide (NHS), rhodamine 110, and cresyl violet 670 are shown in Figures S7, S8, S9, and S10, respectively. The main stretching frequencies are seen in the same location as in the grazing angle spectra for these compounds on modified surfaces. It is noted that grazing incidence IR is dependent on the orientation of a bond relative to the surface, and only those vibrations with transition dipoles perpendicular to the surface will absorb strongly and be observed by the technique. Therefore, certain signals may be observed in an IR spectrum of a solid sample of a compound, however once the compound is attached to a metal surface some signals may not be present due orientation of individual bonds relative to the substrate.

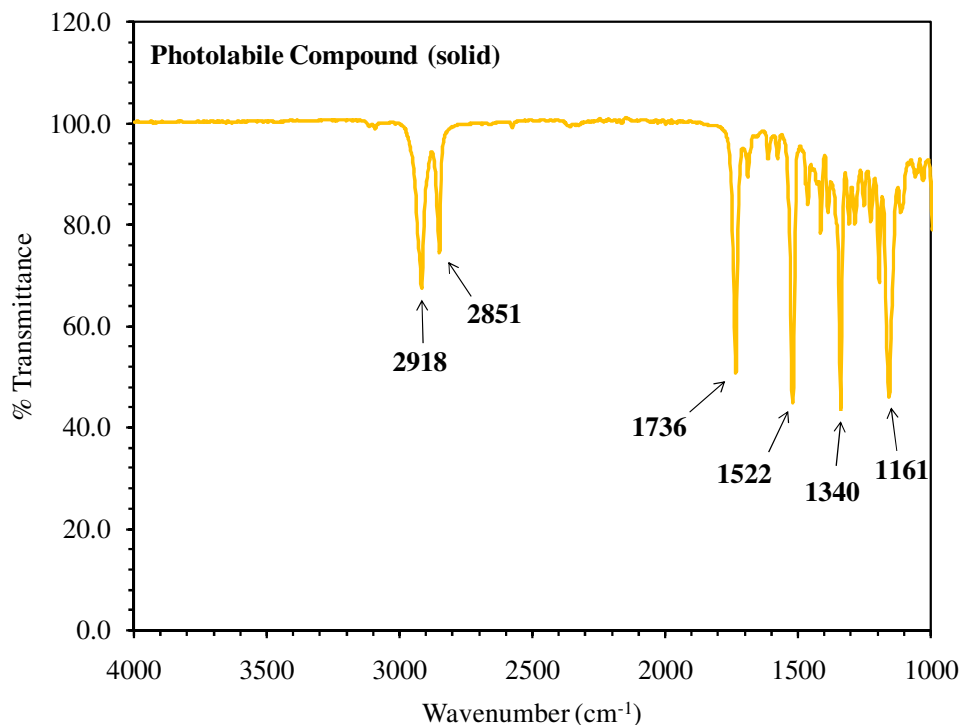


**Figure S7: ATR IR spectrum of solid 2-nitrobenzyl-11-mercaptoundecanoate (photolabile compound).**



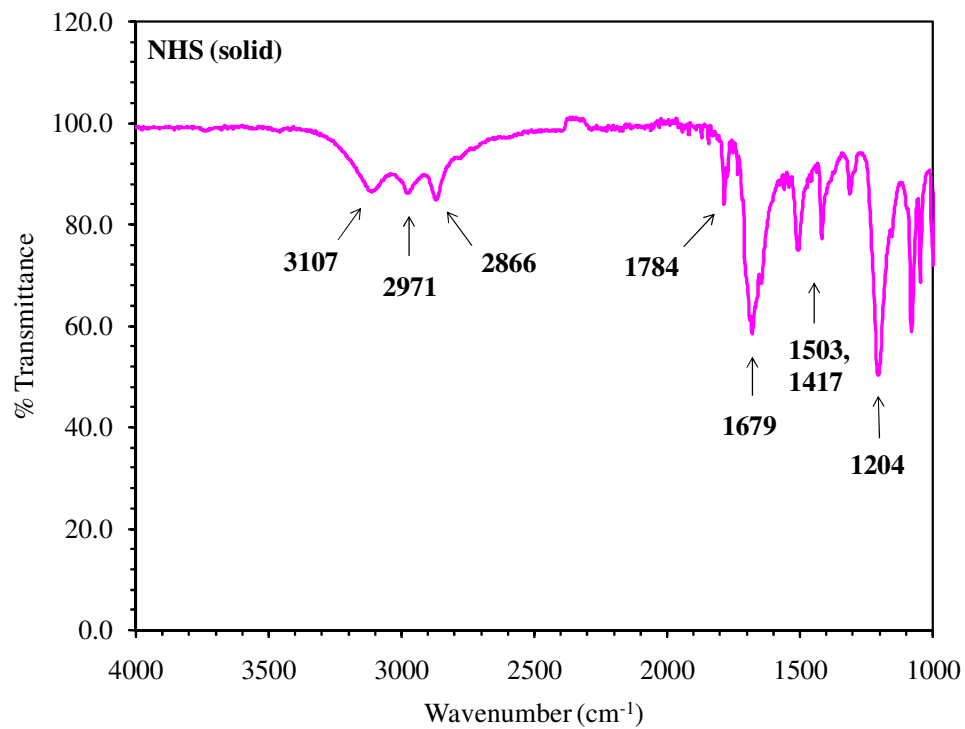


**Figure S8: ATR IR spectrum of solid n-hydroxysuccinimide (NHS).**

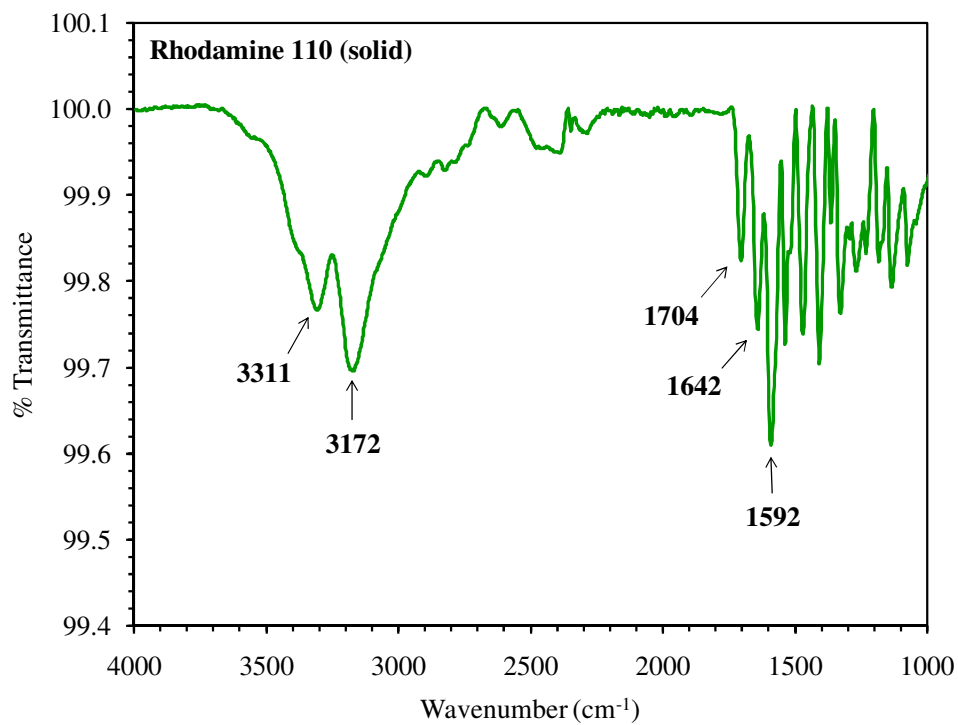


**Figure S9: ATR IR spectrum of solid rhodamine 110.**

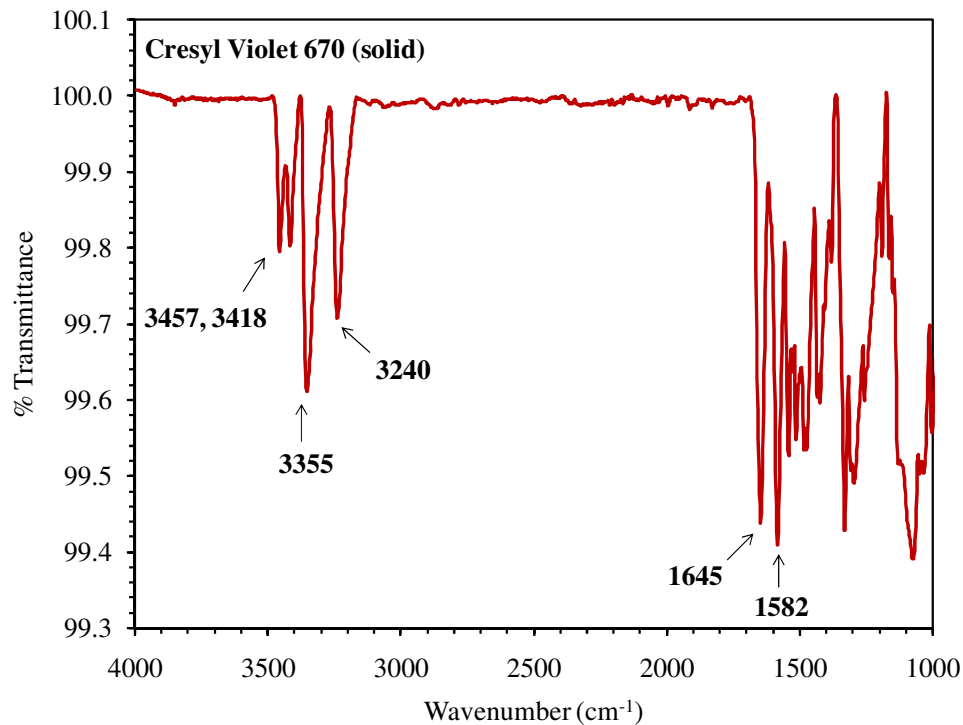


**Figure S10: ATR IR spectrum of solid cresyl violet 670.**

#### *Cyclic Voltammetry.*

Cyclic voltammetry was used to confirm the formation of a well ordered monolayer and that a highly ordered film remained on the surface after each modification step. CV curves for the SAM/irradiated SAM, an EDC/NHS activated surface, a surface functionalized with rhodamine 110, and a surface functionalized with cresyl violet 670 are shown in Figures S11, S12, S13, and S14, respectively. Each graph contains the CV profile of a bare gold substrate for comparison. Attenuation of current for the redox process of ferricyanide in solution is indicative of the presence of an insulating, well ordered film on the metal surface. CVs after each modification step confirm the presence of an insulating monolayer, and demonstrate that the

activation and subsequent amide bond formation steps proceed as expected. The increase in current in comparison to the monolayer seen for each subsequent film is likely due to a reorganization of the SAM following exposure to water during the activation step. The shift of the current peaks to a larger separation than 59 mV, as seen for a reversible process, indicate that slow electron penetration through the layer is occurring, likely due to this reorganization process.

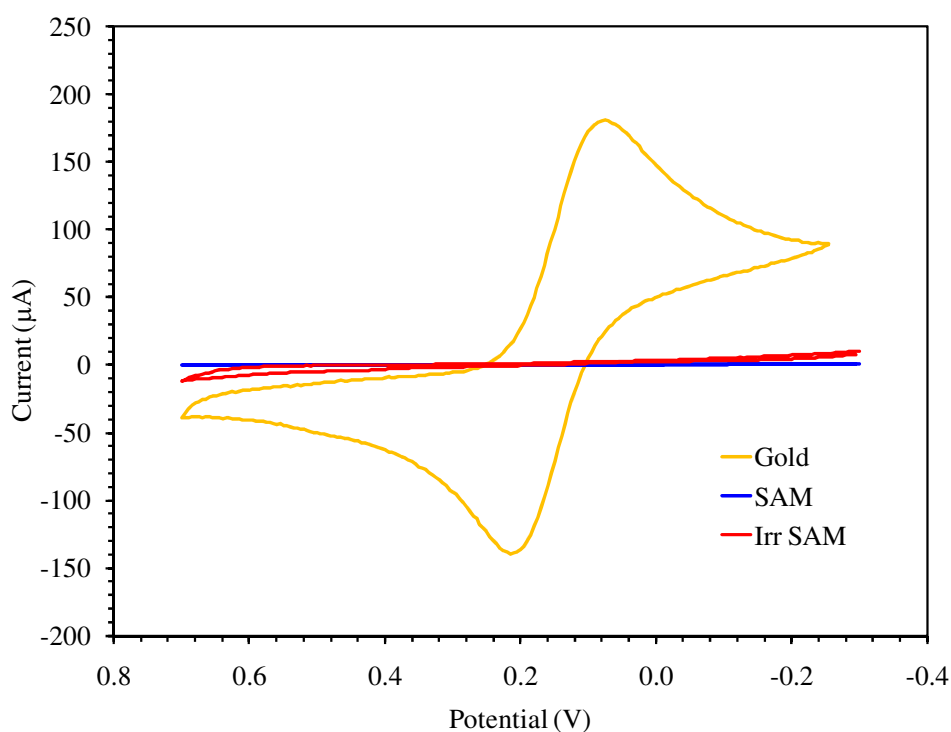


**Figure S11: CV analysis of the SAM and irradiated SAM.**

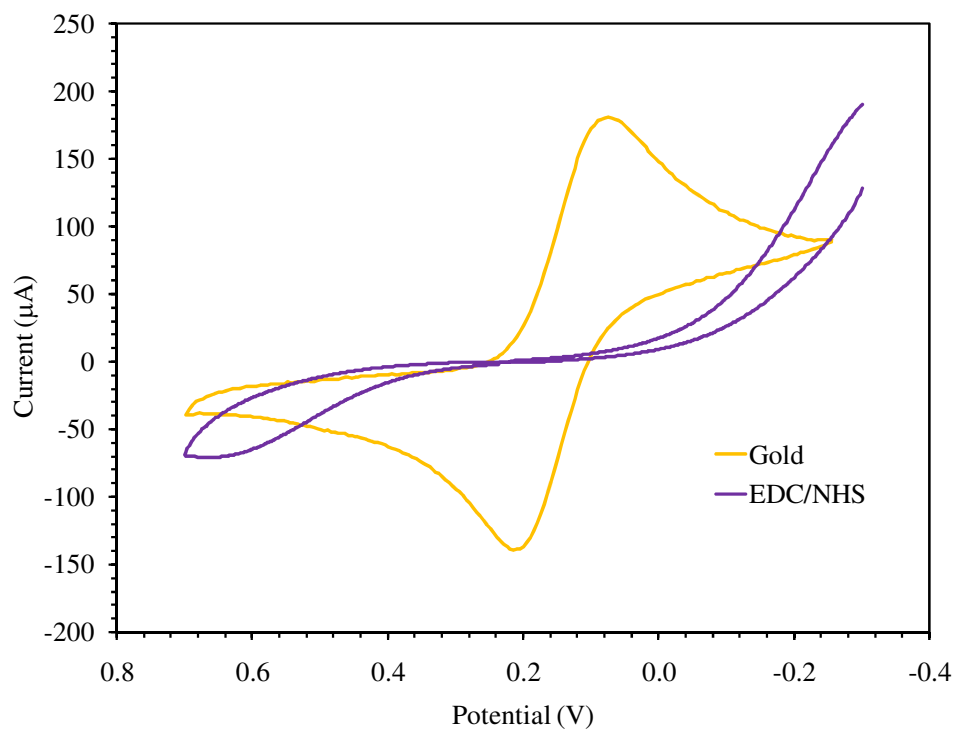


**Figure S12: CV analysis of a SAM activated with EDC/NHS.**

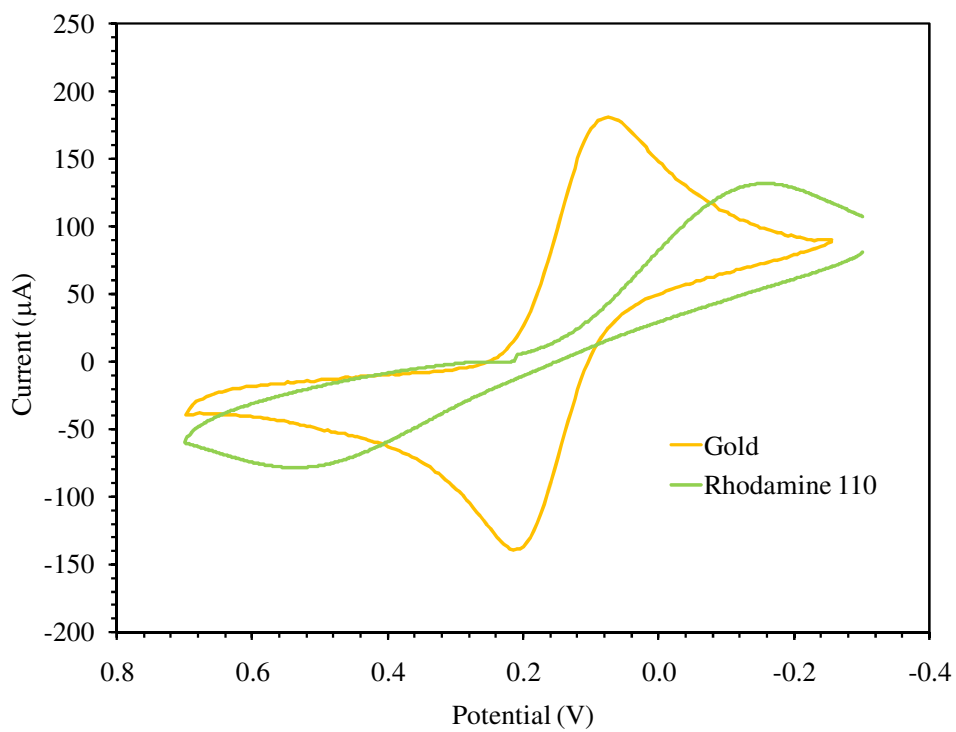


**Figure S13: CV analysis of rhodamine 110 covalently coupled to a SAM.**

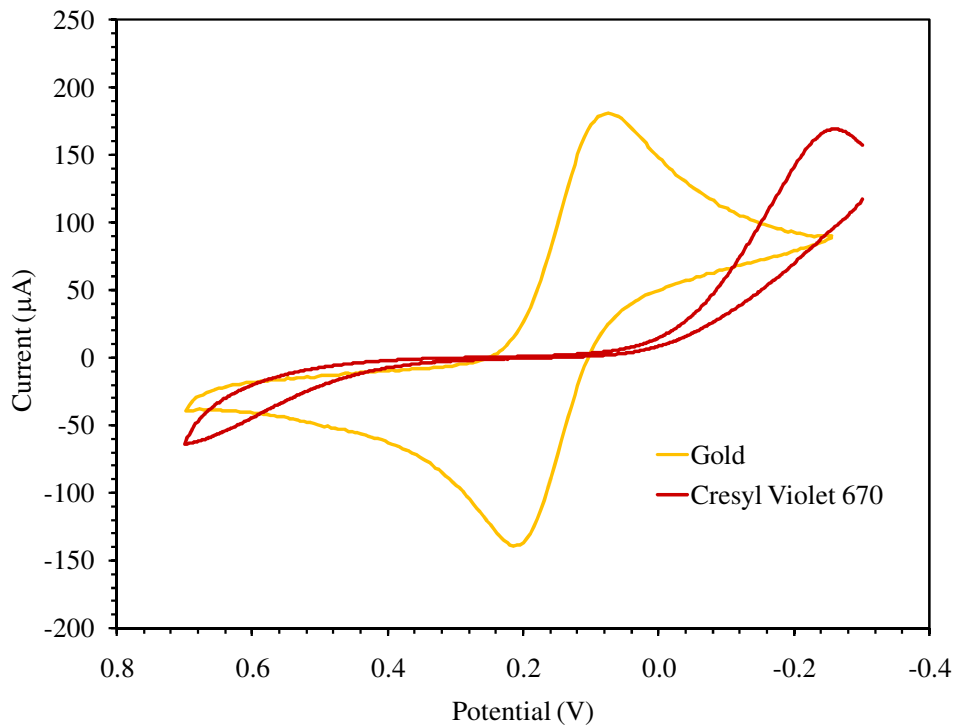


**Figure S14: CV analysis of cresyl violet 670 covalently coupled to a SAM.**

#### *XPS Analysis.*

Complete XPS survey spectra for bare gold, a SAM of the photolabile compound, and irradiated SAM of the photolabile compound are shown in Figures S15, S16, and S17, respectively. This data was used to generate the elemental percentages listed in the tables presented in the body of the paper. XPS confirms successful SAM deposition and protecting group removal after irradiation. As previously mentioned, the Sn and I signals seen in the all of the XPS experiments arise from the gold substrate (see Figure S15) and are due to the preparation of the glass backing used for metal film deposition.

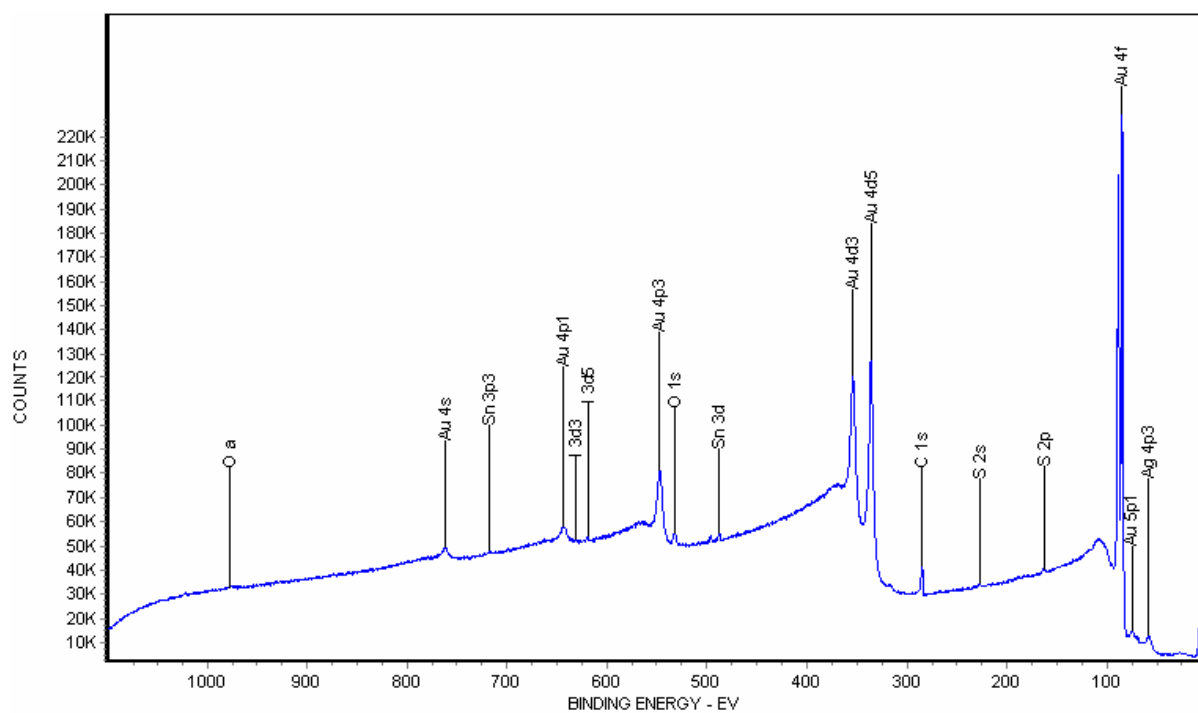


**Figure S15: XPS Spectrum of a bare gold substrate.**

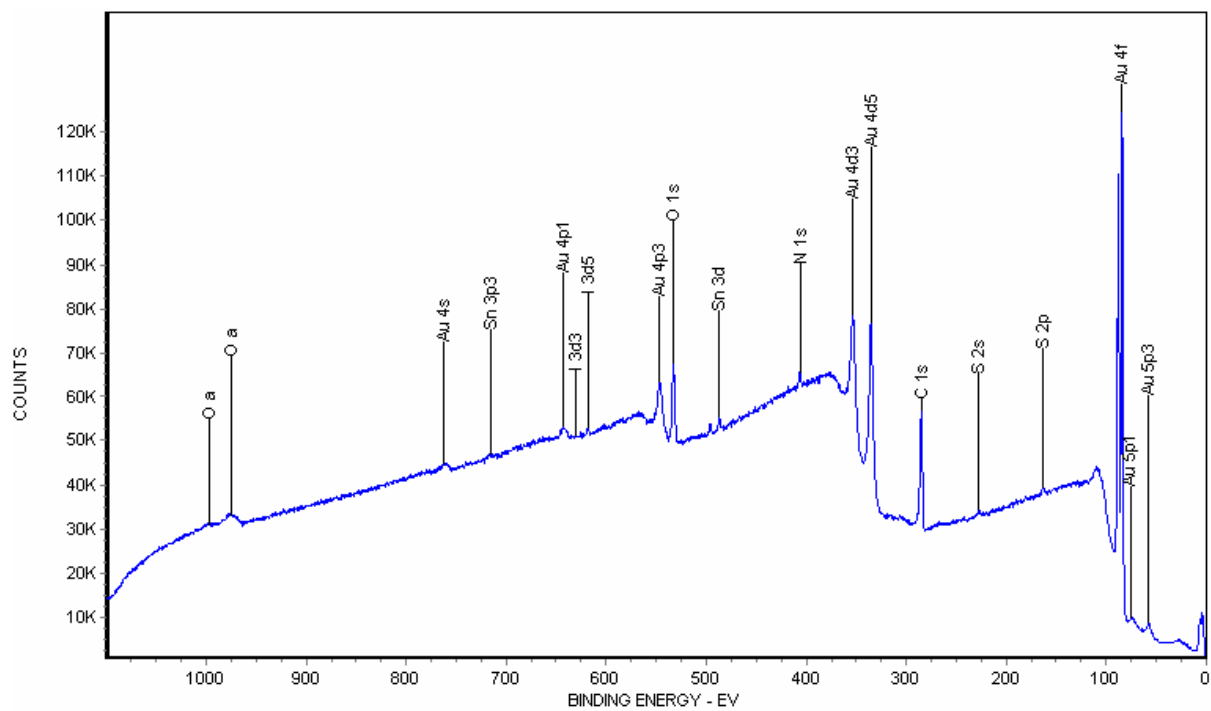


**Figure S16: XPS Spectrum of SAM of the photolabile compound.**

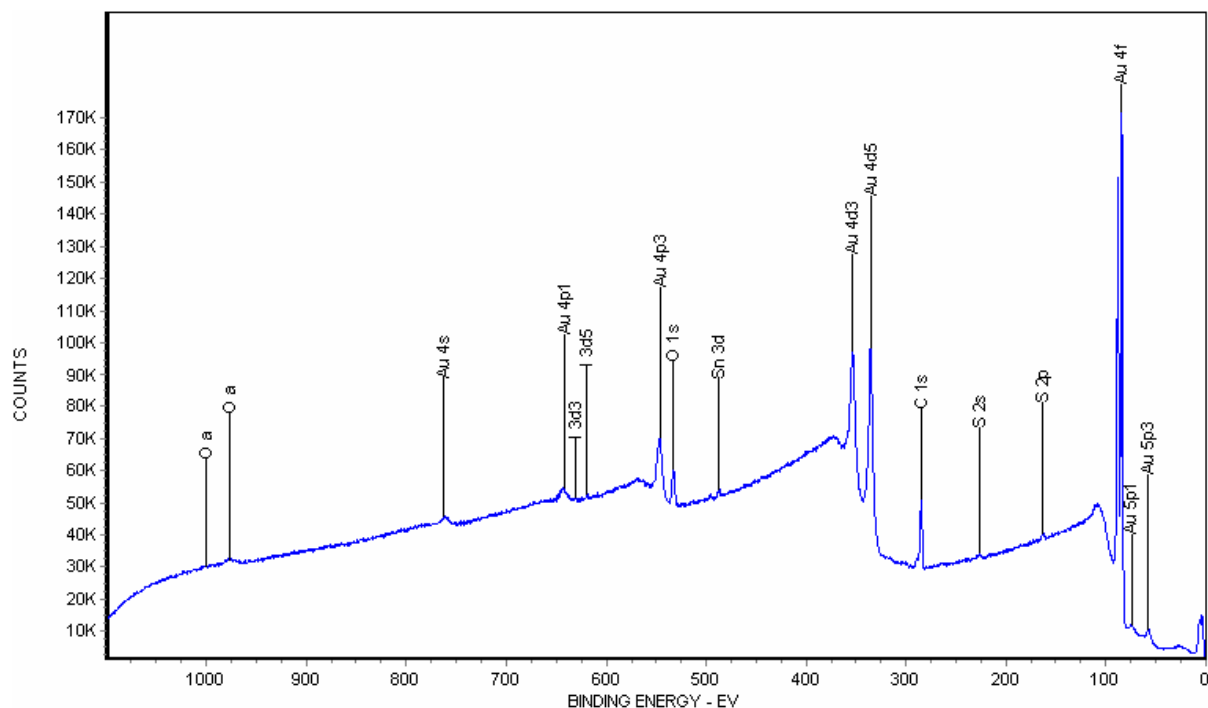


**Figure S17: XPS of irradiated SAM of the photolabile compound.**

#### References.

- (1) Porter, M. D.; Bright, T. B.; Allara, D. L.; Chidsey, C. E. D. *J. Am. Chem. Soc.* **1987**, *109*, 3559-3568.
- (2) Lahiri, J.; Isaacs, L.; Tien, J.; Whitesides, G. M. *Anal. Chem.* **1999**, *71*, 777-790.
- (3) Moraillon, A.; Gouget-Laemmel, A. C.; Ozanam, F.; Chazalviel, J. N. *J. Phys. Chem. C* **2008**, *112*, 7158-7167.
- (4) Voicu, R.; Boukherroub, R.; Bartzoka, V.; Ward, T.; Wojtyk, J. T. C.; Wayner, D. D. M. *Langmuir* **2004**, *20*, 11713-11720.
- (5) Xiao, S.-J.; Brunner, S.; Wieland, M. *J. Phys. Chem. B* **2004**, *108*, 16508-16517.